Detection and characterization of precipitation extremes and geohydrological hazards over a transboundary Alpine area based on different methods and climate datasets

Supplementary material

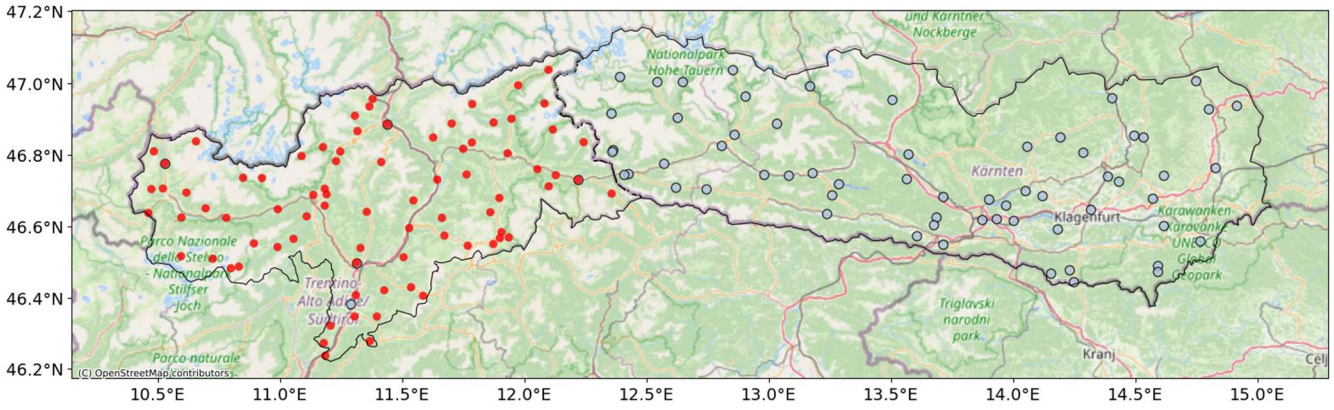

Figure S1: Map with station locations used in SPARTACUS (grey dots) and TST (red dots). Red points with black borders are stations in common. The basemap is taken from ©OpenStreetMap distributed under the Open Data Commons Open Database License (ODbL) v1.0.

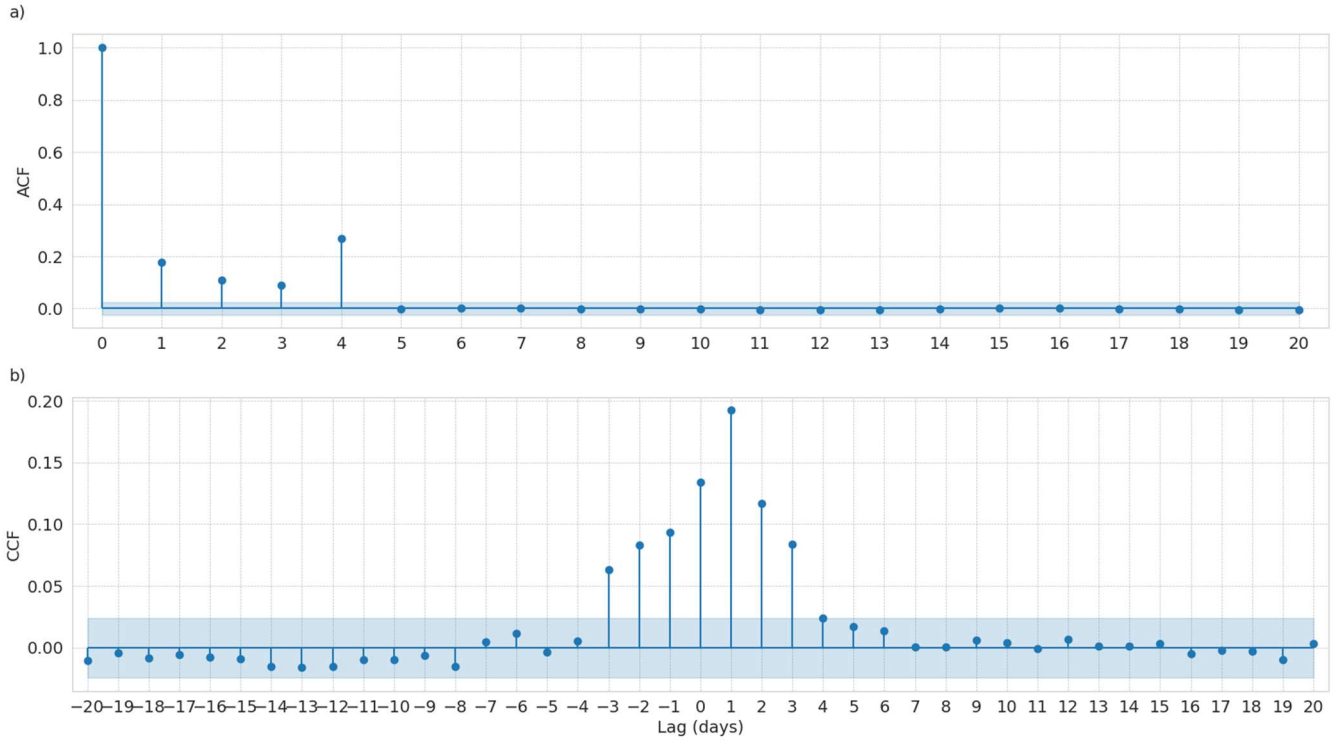

Figure S2: a) Autocorrelation of hazard time series over 2003 to 2020; b) Cross-correlation of normalized and detrended time series of daily hazard records and the local 99th percentile of daily precipitation fields from 2003 to 2020 based on SPARTACUS-TST. The shaded area represents the 0.05 significance threshold.

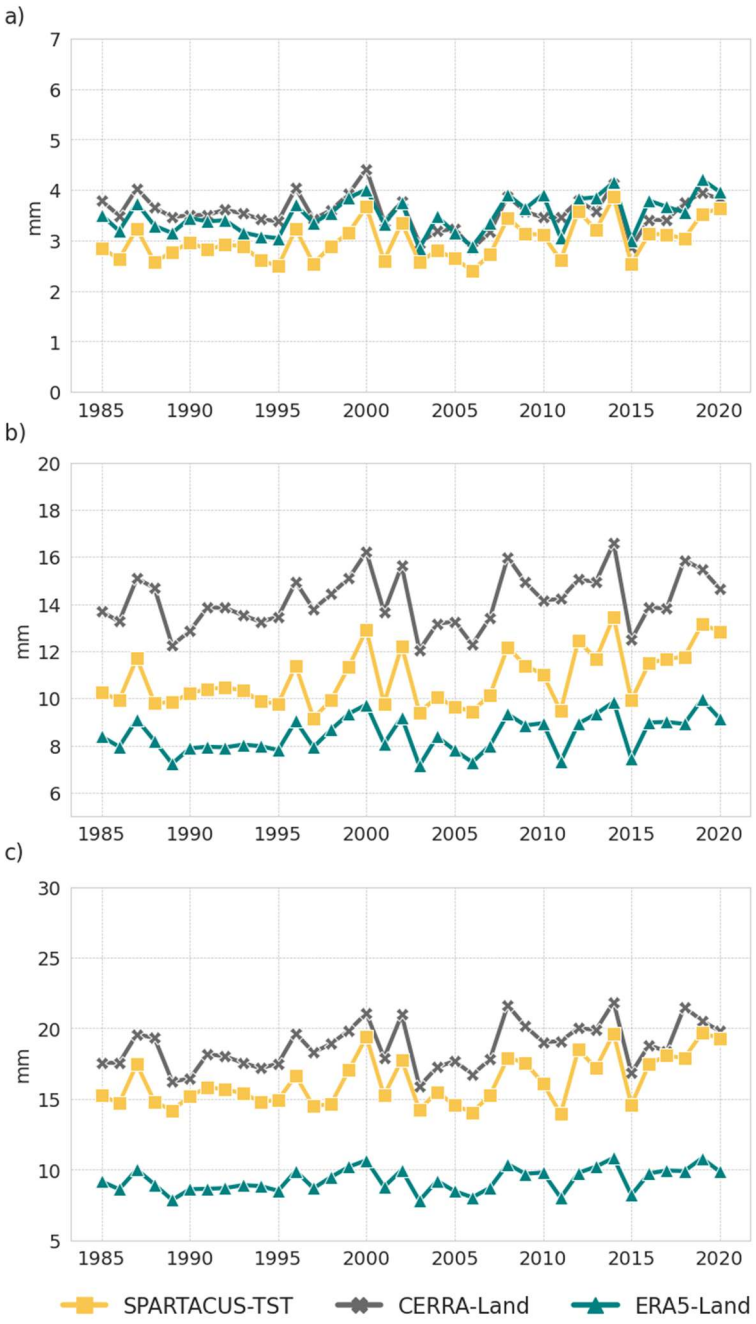

Figure S3: Annual time series 1985-2020 of the yearly averages of daily precipitation statistics: a) areal mean, b) local 99th percentile and c) local maximum over the study region based on SPARTACUS-TST, CERRA-Land and ERA5-Land.

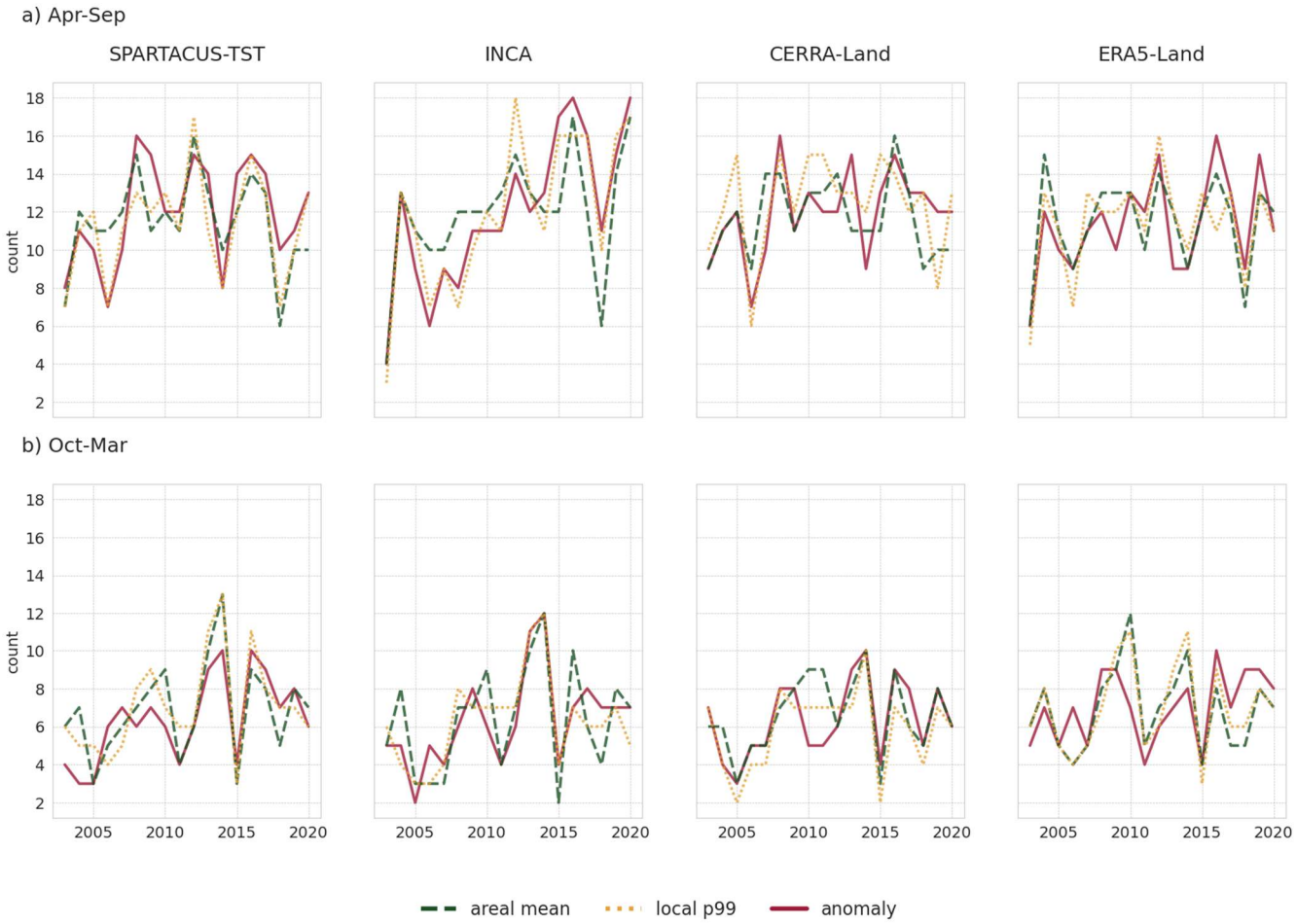

Figure S4: Event counts per year in a) summer half year (April to September) and b) winter half year (October to March) based on the top 5 % most extreme precipitation days detected by different methods from 2003-2020 for SPARTACUS-TST, INCA, CERRA-Land and ERA5-Land.

	areal mean	local p99	anomaly
SPARTACUS-TST	0.21	0.19	0.22
INCA	0.20	0.18	0.21
CERRA-Land	0.19	0.15	0.22
ERA5-Land	0.16	0.16	0.16

Table S1: Correlation coefficients of daily time series of hazard records and different daily precipitation statistics used to detect extreme precipitation events over 2003-2020 for each dataset. The correlation is calculated for all years considering a lag of one day between precipitation statistics and hazard counts.

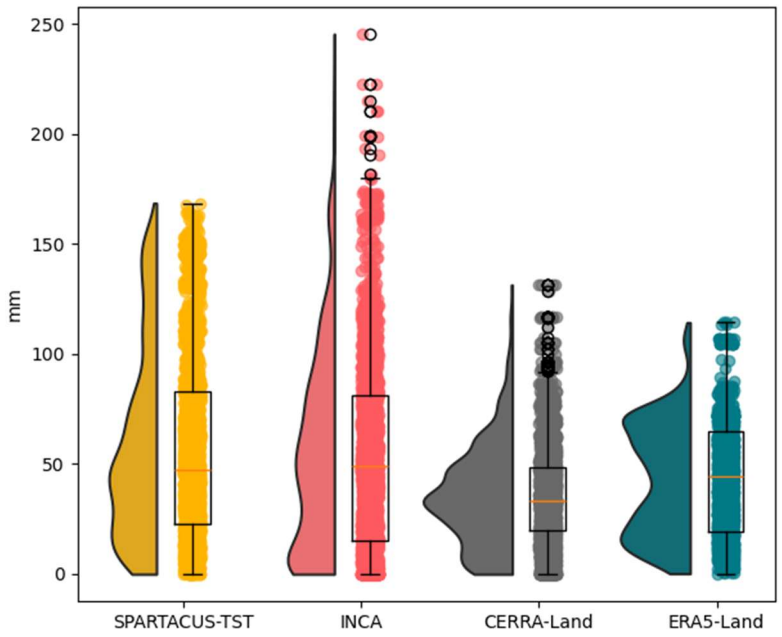

Figure S5: Distribution of 1-day precipitation intensities in the spatial proximity of recorded hazards for all datasets based on the most intense 5 % precipitation events (330 events) detected by the local p99 method. The precipitation intensities are extracted from the closest grid point to each hazard location without averaging over co-occurring hazards.

dataset	method	mean [mm]	median [mm]	75th percentile [mm]	max [mm]	absolute max [mm]
SPARTACUS -TST	local p99	29.6	25.8	40.7	156.9	168.6
	areal mean	29.5	24.7	39.7	156.9	168.6
	anomaly	29.1	24.7	39.6	156.9	168.6
INCA	local p99	29.8	23.7	44.4	151.2	245.5
	areal mean	30.2	25.1	43.4	124.1	177.8
	anomaly	29.0	24.5	43.1	124.1	177.8
CERRA-Land	local p99	23.9	21.9	34.0	99.8	131.4
	areal mean	26.1	23.7	34.5	99.8	142.4
	anomaly	24.4	22.3	33.7	99.8	142.4
ERA5-Land	local p99	23.3	20.4	29.3	76.2	114.3
	areal mean	23.9	20.9	29.4	83.6	98.8
	anomaly	23.8	21.2	29.5	83.6	98.8

Table S2: Summary statistics for mean daily precipitation intensity in the proximity of hazard records (2003-2020) based on the 330 precipitation events detected by each dataset-method combination. Statistics is calculated over precipitation intensities extracted from the closest grid point to each hazard location and averaged over all hazard records on the same date. In the last column the absolute maxima of local intensities without averaging are reported.

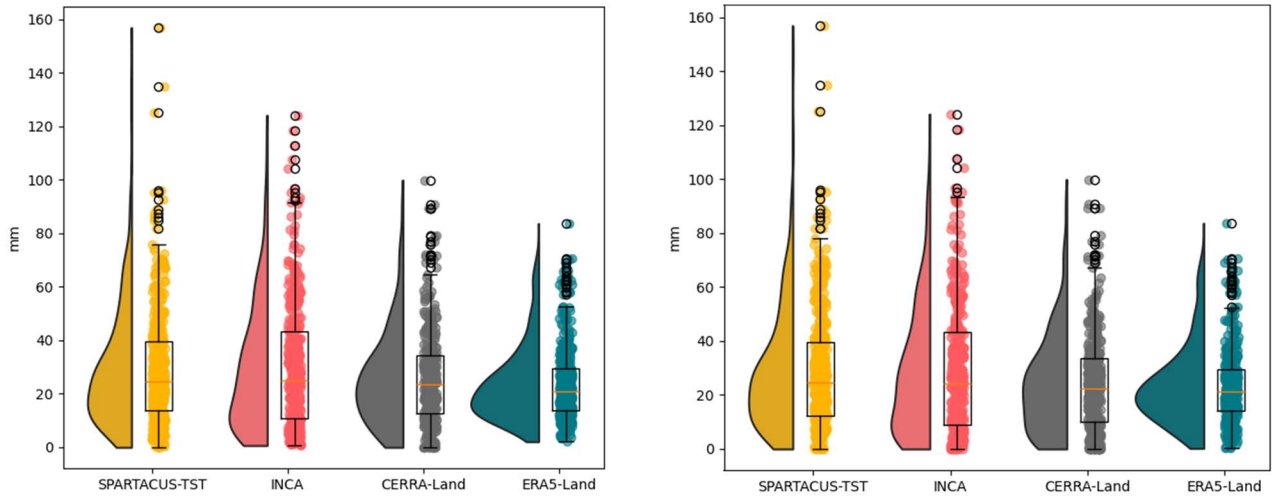

Figure S6: Distribution of 1-day precipitation intensities in the spatial proximity of recorded hazards for all datasets based on the most intense 5 % precipitation events (330 events) detected by the areal mean (left panel) and the anomaly method (right panel). The precipitation intensities are extracted from the closest grid point to each hazard location and averaged over all hazard records on the same date.

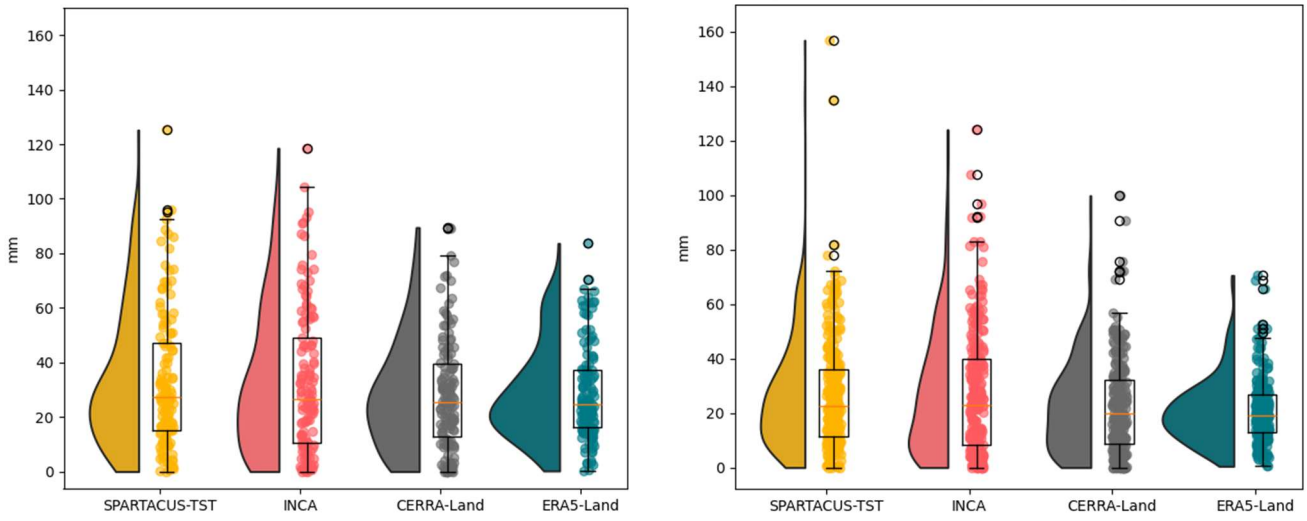

Figure S7: Distribution of precipitation intensities in the spatial proximity of recorded hazards for all datasets for the winter half year (October to March, left panel) and the summer half year (April to September, right panel) detected by the local p99 method. The precipitation intensities are extracted from the closest grid point to each hazard location and averaged over all hazard records on the same date.